ORIGINAL PAPER

Preparation and characterization of blended solid polymer electrolyte 49% poly(methyl methacrylate)-grafted natural rubber:poly(methyl methacrylate)–lithium tetrafluoroborate

M. S. Su'ait · S. A. M. Noor · A. Ahmad · H. Hamzah · M. Y. A. Rahman

Abstract The preparation and characterization of blended solid polymer electrolyte 49% poly(methyl methacrylate)-grafted natural rubber (MG49):poly(methyl methacrylate) (PMMA) (30:70) were carried out. The effect of lithium tetrafluoroborate ($LiBF_4$) concentration on the chemical interaction, structure, morphology, and room temperature conductivity of the electrolyte were investigated. The electrolyte samples with various weight percentages (wt. %) of $LiBF_4$ salt were prepared by solution casting technique and characterized by Fourier transform infrared spectroscopy, X-ray diffraction (XRD), scanning electron microscopy (SEM), and electrochemical impedance spectroscopy. Infrared analysis demonstrated that the interaction between lithium ions and oxygen atoms occurred at symmetrical stretching of carbonyl (C=O) ($1,735$ cm^{-1}) and asymmetric deformation of (O–CH_3) ($1,456$ cm^{-1}) via the formation of coordinate bond on MMA structure in MG49 and PMMA. The reduction of MMA peaks intensity at the diffraction angle, 2θ of $29.5°$ and $39.5°$ was due to the increase in weight percent of $LiBF_4$. The complexation occurred between the salt and polymer host had been confirmed by the XRD analysis. The semi-crystalline phase of polymer host was found to reduce with the increase in salt content and confirmed by XRD analysis. Morphological studies by SEM showed that MG49 blended with PMMA was compatible. The addition of salt into the blend has changed the topological order of the polymer host from dark surface to brighter surface. The SEM analyses supported the enhancement of conductivity with the addition of salt. The conductivity increased drastically from 2.0 to 3.4×10^{-5} S cm^{-1} with the addition of 25 wt.% of salt. The increase in the conductivity was due to the increasing of the number of charge carriers in the electrolyte. The conductivity obeys Arrhenius equation in higher temperature region from 333 to 373 K with the pre-exponential factor σ_o of 1.21×10^{-7} S cm^{-1} and the activation energy E_a of 0.46 eV. The conductivity is not Arrhenian in lower temperature region from 303 to 323 K.

Keywords Solid polymer electrolyte · Ionic conductivity · 49% Poly(methyl methacrylate)-grafted natural rubber (MG49) · Poly(methyl methacrylate) (PMMA) · Lithium tetrafluoroborate ($LiBF_4$)

M. S. Su'ait · A. Ahmad · H. Hamzah
Polymer Research Center, Faculty of Science and Technology,
Universiti Kebangsaan Malaysia,
43600 Bangi, Selangor, Malaysia

M. S. Su'ait · A. Ahmad · H. Hamzah
School of Chemical Sciences and Food Technology,
Faculty of Science and Technology,
Universiti Kebangsaan Malaysia,
43600 Bangi, Selangor, Malaysia

M. Y. A. Rahman
College of Engineering, Universiti Tenaga Nasional,
43009 Kajang, Selangor, Malaysia

S. A. M. Noor · A. Ahmad (✉) · M. Y. A. Rahman (✉)
Chemistry Department, Center for Defence Foundation Studies,
National Defence University of Malaysia,
57000 Kuala Lumpur, Malaysia
e-mail: azizan@ukm.my
e-mail: yusri@uniten.edu.my

Introduction

Over the last three decades, the growth of research on rechargeable batteries becomes very important in the field of power sources. Rechargeable batteries become a leading power source and the heart of modern advances in portable energy sources, electrochemical devices, photo-electrochemical cell,

electric vehicle, and hybrid electric vehicle. Solid polymeric electrolyte (SPE)-containing dissolved inorganic salts have received much attention because the electrolyte materials are one of the promising candidates for use in solid-state rechargeable lithium batteries and other ionic devices. SPE possesses many advantages over liquid electrolyte in terms of shape, geometry, mechanical strength, and good electrode–electrolyte contact [1]. Polymer electrolyte was first discovered by Fenton et al. in 1973 [2]. They reported that poly(ethylene oxide) (PEO)–salt complexes can exhibit ionic conductivity at room temperature. Since then, there has been substantial research activity towards the preparation of a various type of polymer electrolytes for Li-based batteries having different combinations of polymer and salts [3–7]. Poly(methyl methacrylate) (PMMA) with its structure shown in Fig. 1 has been used as a polymer host due to its high transparency in the visible region as preferred solid electrolyte in electro-chromic window [8], high stability at lithium–electrolyte surface [9], and able to be diluted by various organic solvents [10]. PMMA-based electrolyte is also less reactive for lithium electrode. Therefore, it is expected that a higher reproducibility of lithium electrode in battery utilizing PMMA-based electrolyte [11]. To enhance the room temperature conductivity of electrolyte, various modifications have been proposed, such as incorporating inorganic oxide and ceramic filler, cross-linking, and blending with different polymers and plasticizers into conventional electrolyte systems [12–14]. Apart from improving ionic conductivity, it is also necessary to preserve the mechanical stability of electrode–electrolyte interface, which also acted as separator that insulates the positive electrode from the negative. The sufficient mechanical strength was required to withstand the electrode stack pressure and stresses caused by dimensional changes that the rechargeable electrodes undergo during charge/discharge cycling [10]. The mechanical properties of polymer electrolyte can be improved by increasing the polymer/solvent ratio, which adversely affects the ionic conductivity of the polymer electrolyte system [15]. An alternative to plasticizers and ceramic fillers is to blend it with elastomeric polymer such as modified natural rubber [16]. This is because of their distinctive characteristics such as low glass transition temperature, soft elastomeric characteristics at room temperature, good elasticity, and adhesion that make them a suitable candidate as a polymer host for polymeric electrolyte system
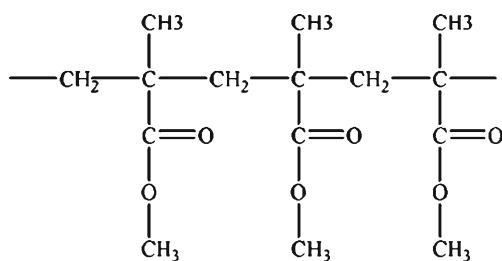
[17]. The good elasticity and adhesion properties of modified natural rubber will provide efficient contact between the electrodes in electrochemical devices [17]. Furthermore, modified natural rubber such as 49% grafted poly(methyl methacrylate) (MG49) with its structure shown in Fig. 2 have a polar group in their carbonyl functional group that will provide coordination sites for Li$^+$ conduction [18–23]. In addition, the use of modified natural rubber will produce the electrolyte that is low in cost and environmental friendly. The blended PMMA:MG49 electrolyte system is expected to provide good electrode–electrolyte contact and mechanical property to the electrolyte since PMMA acts as a stiffener promoting fast ion transport through a continuous conduction path that does not affect the electrochemical stability of the electrolyte [24].

This paper describes the preparation of (30:70) MG49:PMMA-based polymer electrolyte doped with various weight percentages lithium tetrafluoroborate (LiBF$_4$) by solution casting technique. The samples were characterized by Fourier transform infrared spectroscopy (FTIR), X-ray diffraction (XRD), scanning electron microscopy (SEM), and electrochemical impedance spectroscopy (EIS). It is expected that the addition of LiBF$_4$ salt will improve the ionic conductivity of MG49:PMMA solid polymer electrolyte. The variation of electrolyte conductivity with temperature was also investigated.

Methodology

Reagent and sample preparation The starting materials are PMMA with low molecular weight and LiBF$_4$ salts supplied by Fluka chemicals. MG49 was commercially obtained from Green HPSP (Malaysia) Sdn. Bhd. Technical grade organic solvent, tetrahydrofuran (THF), and toluene were purchased from SYSTERM® ChemAR®-Kielce, Poland. MG49 was dissolved in stopped flasks containing toluene. After 24 h, the solution was stirred with efficient magnetic
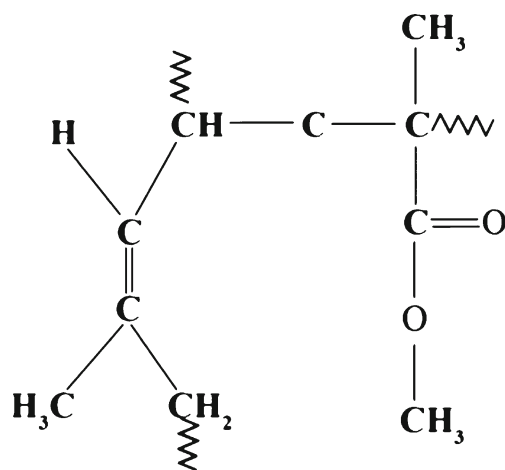

Fig. 1 Structure of PMMA

Fig. 2 Structure of MG49 monomer

stirring for the next 24 h until complete dissolution of MG49 into clear viscous solution. PMMA solution was prepared in another stopped flask containing toluene and stirred for 24 h. These two solutions were then mixed for 24 h to obtain a homogenous solution. LiBF$_4$ salt was dissolved in THF solution and stirred for 12 h. The solution was added to the previous solution and continuously stirred for the next 24 h to obtain a homogenous solution. The electrolyte solution was then cast onto a glass petri dish and the solvent was allowed to slowly evaporate in a fume hood at room temperature. A free standing film was obtained when the solvent evaporated completely. Residual solvent was then removed in a vacuum oven at 50 °C for 48 h. The samples were then stored in a desiccator until further testing. The same experimental procedure was repeated for preparing the electrolytes with different weight percent of salt. The temperature dependence on conductivity was performed in a temperature range 303 to 373 K.

Sample characterization FTIR spectroscopy was used to observe the vibration energy of covalent bond in the polymer host, and the interaction occurs with the presence of salt addition. FTIR spectrum was recorded by computer-interfaced Perkin Elmer GX Spectrometer. The electrolyte sample was cast onto NaCl windows and was analyzed in the frequency range of 4,000 to 400 cm^{-1} with the scan resolution of 4 cm^{-1}. XRD model D-5000 Siemen was used to observe the appearance and disappearance of crystalline or amorphous phase with the addition of salt. The structural studies of the solid polymer electrolyte samples were investigated by XRD analysis from the range of diffraction angle, 2θ from 2° to 80° at rate 0.04°s^{-1}. The morphology of the samples was observed by SEM model Philips XL30 with ×1,000 magnification at 20 kV electron beam. The sample was fractured in liquid nitrogen and coated with gold sputter-coated machine before the analysis. The conductivity measurements were carried out by EIS using high-frequency resonance analyzer model 1255 with applied frequency from 6,500 to 0.1 Hz at perturbation voltage of 1,000 mV. The disc-shaped sample of 16 mm in diameter was sandwiched between two stainless steel block electrodes. The analysis was conducted at room temperature.

Results and discussion

Infrared Figure 3 shows the FTIR spectrum of MG49: PMMA–LiBF$_4$. Since each type of bonds has a different natural frequency of vibration, the identification of absorption peak in the vibration portion of infrared region l gives a specific type of bonding [25, 26]. The main interests are shown on the oxygen atoms of the carbonyl (C=O) (1,750–1,730 cm^{-1}) and ether group (C–O–C) (1,300–1,000 cm^{-1})
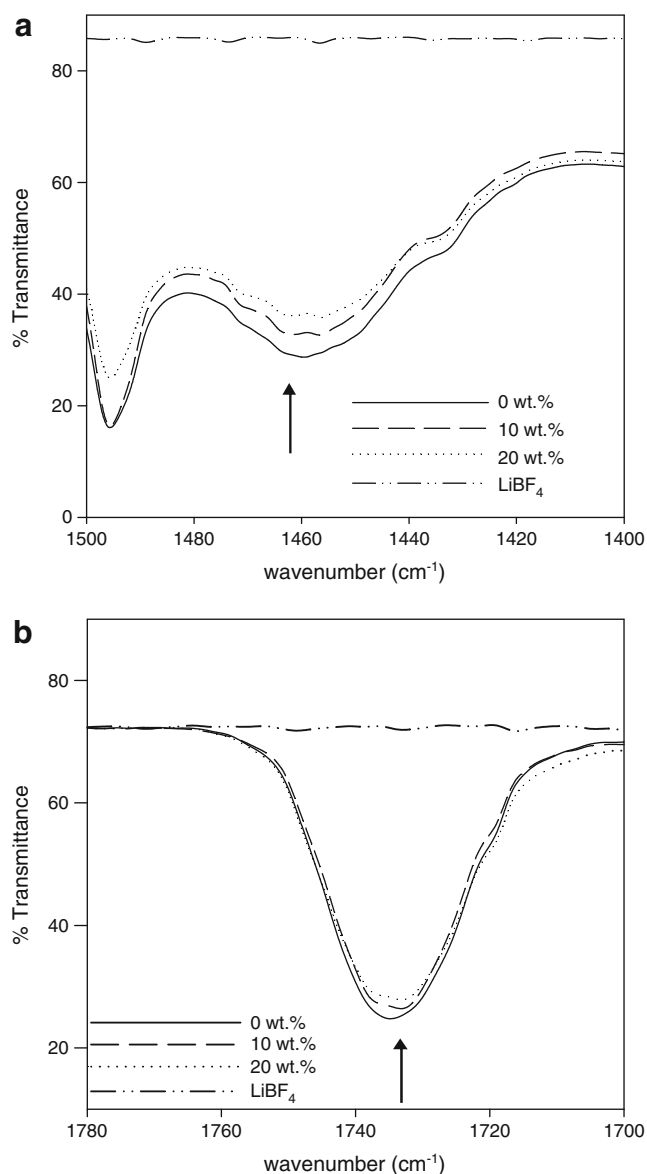
Fig. 3 **a** FTIR spectrum of MG49:PMMA–LiBF$_4$ for δ(O–CH$_3$). **b** FTIR spectrum of MG49:PMMA–LiBF$_4$ for v (C=O)

from PMMA and MG49 [25]. These regions show significant changes because if the cations were coordinated with the ether oxygen, changes in the ether oxygen vibration modes are expected to be observed [27]. The oxygen atom at the C–O–C and C=O functional group carries lone pairs of electron that are donated to Li$^+$ ions from the lithium salt to form polymer–salt complexes via dative bond [21, 23, 28]. The C=O symmetrical stretching frequency of MMA from polymer host, MG49:PMMA gives rise to an intense, very strong, and sharp peak at 1,732 cm^{-1}. With the addition of salt, the intensity of C=O symmetric stretching of MMA peak is reduced and shifted to the lower wavenumber from 1,732 to 1,735 cm^{-1}. A shift at δ(O–CH$_3$) asymmetric deformation of MMA from 1,461 to 1,456 cm^{-1} in Fig. 3a

was also observed. Furthermore, the intense, strong, and sharp peak became weak and broader with the addition of lithium salt as shown in Fig. 3a, b. The reduction of peak intensity and the shift of C=O symmetric stretching of MMA peak are demonstrated in Fig. 3b. The previous study reported that the shift of the intensity peaks still occur even though in an insignificant range [20]. The shift of the intensity peaks confirmed the interaction between Li$^+$ ions from doping salt and oxygen atoms in the structure of polymer host to form a coordinate bond and subsequently forming polymer–salt complexes. It was also observed that there are no significant changes at C=C stretching of polyisoprene at 1,604 cm^{-1}. This shows that the interaction between Li$^+$ ions and electron donor atoms only affects the bonding within polar group in polymer host.

X-ray diffraction The XRD patterns of solid polymer electrolyte MG49:PMMA films with various concentration of LiBF$_4$ and pure LiBF$_4$ salt are shown in Fig. 4. The characteristics peak of LiBF$_4$ salt can be observed at the diffraction angle, 2θ of 13.5°, 18.8°, 21.5°, 23.6°, 26.8°, 28.2°, 32.0°, 32.8°, 36.4°, 37.5°, 38.3°, 39.9°, 44.6°, 50.5°, and 54.9°. Feature of semi-crystalline peak for MMA in blended PMMA-MG49 can be observed at the presence of hump in the range between 10° and 25° and MMA single peak at 29.5°, 47.6°, and 48.6° corresponds to MMA. The reduction of intensities and the broadening of the hump by increasing the wt.% of salt indicates that the complexation has taken place, thus decreased the semi-crystalline phase of MMA peak. Furthermore, the MMA single peak at 29.5°, 47.6°, and 48.6° corresponds to MMA group reduced with the addition of LiBF$_4$ salts, thus increased the ionic conductivity of the MG49–PMMA systems [24, 29, 30]. The degree of

crystallinity of MMA also decreases with the LiBF$_4$ content. However, the appearance of LiBF$_4$ peak (13.5°, 23.0°, 31.4°, 35.5°, and 54.9°) at higher wt.% salt showed the salt was recrystallized and associated especially at 15 wt.% LiBF$_4$ salt. The recrystallization of lithium salt is due to the ion association between opposite ionic species in the electrolyte at the high salt concentration [24]. This phenomenon resulted in low electrolyte conductivity to be applied in electrochemical devices even though the addition of lithium salt reaches its maximum level [31]. Nevertheless, this finding was similar to the finding reported elsewhere in which the high ionic conductivity still occurs either by the reduction of crystalline phase or the enhancement of amorphous phase in the polymer host [22, 24, 29, 31].

Scanning electron microscopy Figure 5a, b shows the surface morphology of pure MG49 and PMMA films. Meanwhile, Fig. 5c shows the surface morphology of MG49:PMMA prepared by solution blending method. The homogeneity of MG49:PMMA can be seen as there is no phase separation observed. However, the blended MG49:PMMA shows an uneven and rough surface morphology due to brittle properties of the sample. After the addition of 15 wt.% LiBF$_4$, the surface morphology becomes rougher and the presence of particles shows the recrystallization of salt occur due to excessive amount of LiBF$_4$ in the electrolyte system. This recrystallization contributed to the brittle properties of polymer electrolyte as shown by the crack region in Fig. 5d. Observation on the maximum conductivity shows the absence of lithium salts particle and an increase in the quantity of brightness surface in Fig. 5e. However, the presence of crack region makes the (30:70) MG49:PMMA samples break and split easily [31].

Fig. 4 XRD patterns of solid polymer electrolyte MG49:PMMA films with various concentration of LiBF$_4$
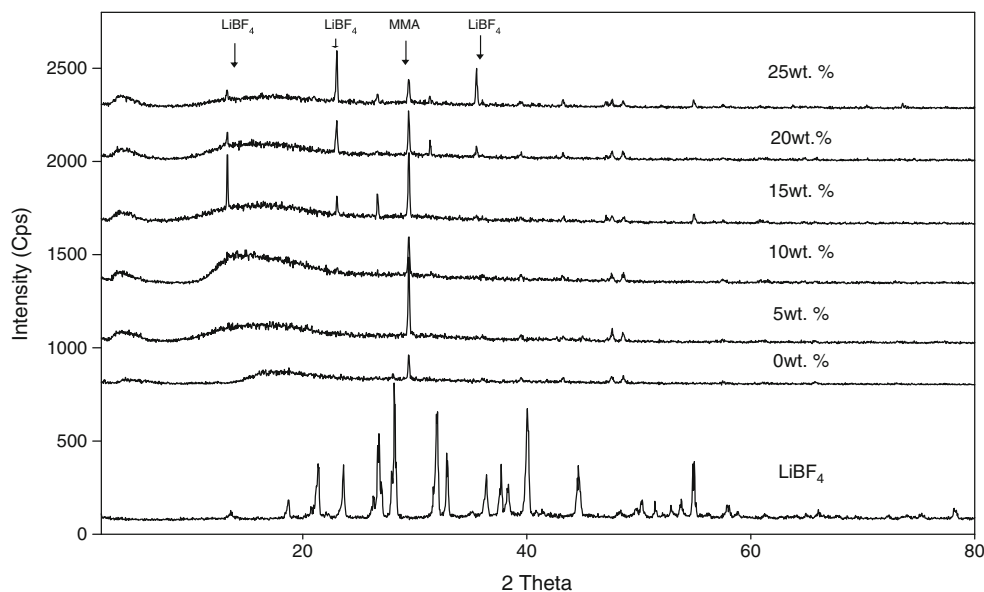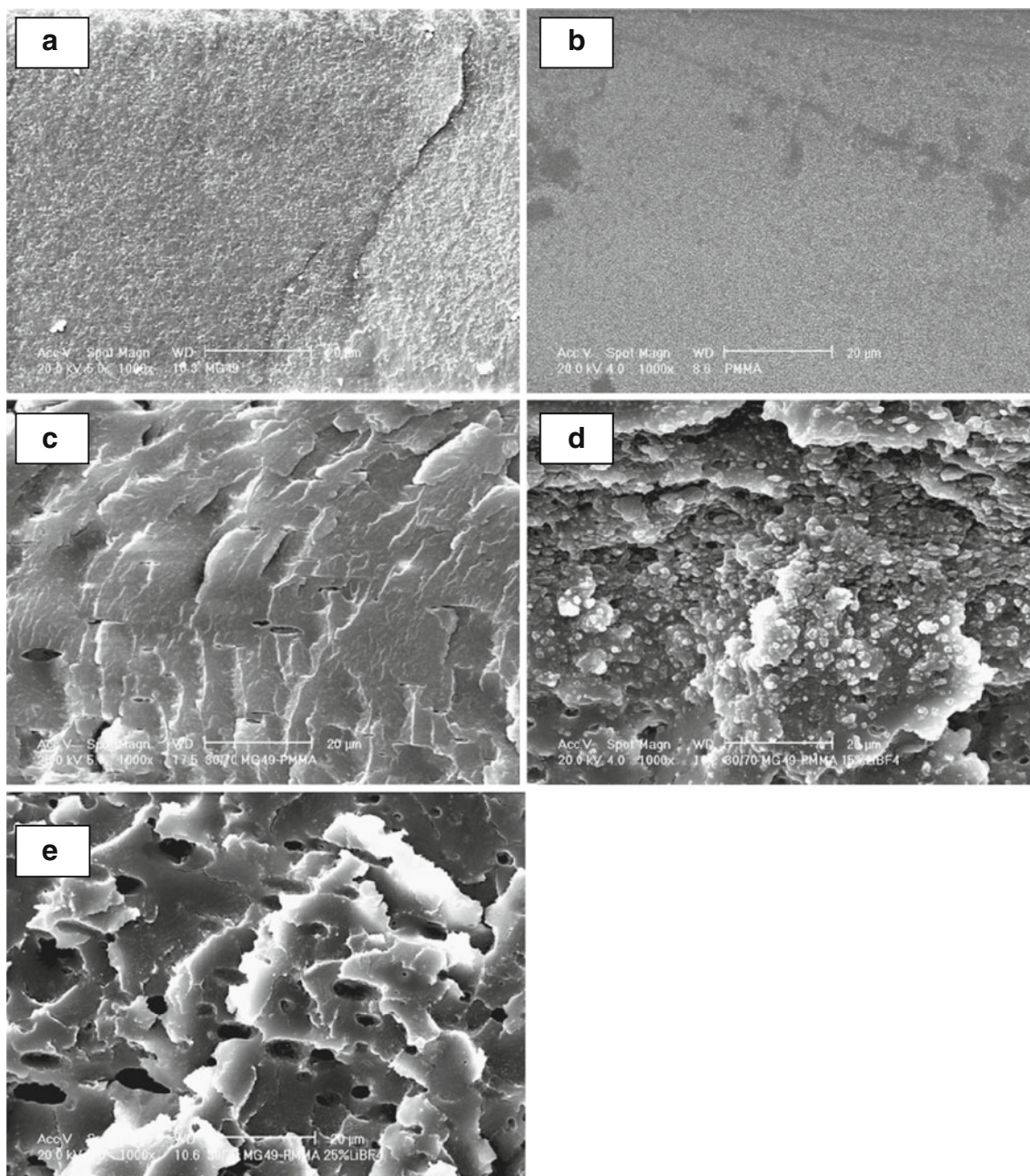
Fig. 5 Micrograph SEM of **a** MG49, **b** PMMA, and MG49:PMMA–LiBF$_4$ at **c** 0 wt.%, **d** 15 wt.%, and **e** 25 wt.%

Ionic conductivity Figure 6 shows the variation of room temperature conductivity of MG49:PMMA–LiBF$_4$ electrolyte with LiBF$_4$ content. The conductivity of MG49:PMMA without LiBF$_4$ is 2.0×10^{-11} S cm^{-1}. The ionic conductivity increased rapidly by three orders of magnitude with the addition of 5 wt.% LiBF$_4$ as Li$^+$ charge carriers were added to the system. It was observed that the ionic conductivity increases drastically apart from region 15 wt.%, up to 25 wt.% LiBF$_4$. The increase in ionic conductivity is due to the increase of the charge carriers in the electrolyte system as given by the proportional relationship between numbers of charges and the conductivity in the following equation: $\sigma = ce(u_+ + u_-) = c\Lambda$, where σ is conductivity, Λ is molar conductivity, c is salt concentration, e is charge on an electron, and u_+ and u_- represent the ion mobility [6]. The maximum conductivity achieved was 3.4×10^{-5} S cm^{-1}. The increase is about $\sim1.9\times10^6$ times higher after the addition of 25 wt.% LiBF$_4$ salt to the blend system. This conductivity was much higher compared with our previous work on MG49–LiBF$_4$ without the presence of PMMA [31]. This observation suggested that PMMA provided an alternative pathway for Li$^+$ ions to transport in polymer segment due to its low dielectric constant as
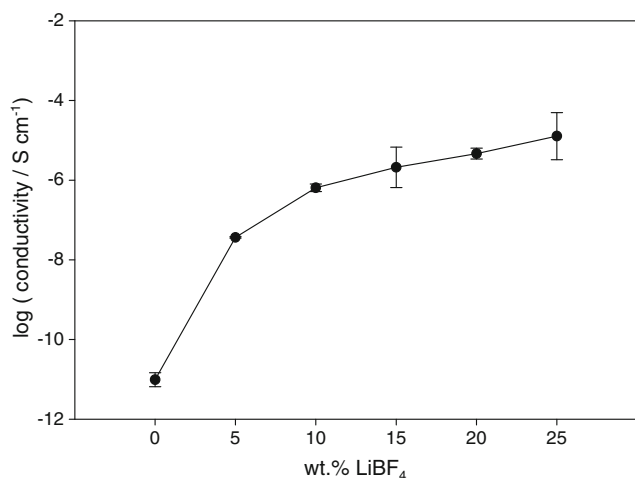
Fig. 6 Variation of room temperature conductivity of MG49:PMMA–LiBF$_4$ with LiBF$_4$ content

compared with MG49. Low dielectric constant helps to increase the degree of ion salvation, thus, leads to dissociation of ionic species. Our previous work on MG49–PMMA–LiClO$_4$ signifies that the size of anion species affects the conductivity of the electrolyte [24]. The size of BF$_4$ anion is known to be larger than ClO$_4$ anion. The large anion size is required for delocalization of ionic charge that could minimize the lattice energy. The smaller size of lithium ions could contribute to the increase of ion dissociation resulted from coulombic interaction forces between lithium cations and large anions [32]. Moreover, this finding almost agrees well with the conductivity found by Wang et al. [33] on PEO–LiBF$_4$ solid polymer electrolytes. The increase in ionic conductivity with the addition of salt is attributed by the increase of charge carriers and reduction of semi-crystalline phase of polymer host as proven by XRD analysis. Although, XRD analysis and SEM observation show the presence of recrystallization phase of LiBF$_4$, this still gives the highest ionic conductivity up to $\sim 10^{-5}$ S cm^{-1}. The high crystallization phase phenomenon was suggested by Bruce in 2005 and reexamined by fellow scientists nowadays [34]. Table 1 shows [O/Li$^+$] ratios at different weight percent of LiBF$_4$ salt. The symbol [O] represents the number of oxygen atoms in both MG49 and PMMA, while [Li$^+$] is the number of lithium cation from the doping

salt. The [O/Li$^+$] ratio for polymer blend was calculated by equation [35, 36]:

$$[O/Li^+] = \frac{M_T \times Mw_s}{M_s \times ((Mw_m/n_m) + (Mw_{PMMA}/n_{PMMA}) + (Mw_{MG49}/n_{MG49}))}$$

where M_T = total mass of the polymer (PMMA + MG49) (in grams), Mw_s = the molecular weight of salt (in grams per mole), M_s = the mass of salt (in grams), Mw_m = the molecular weight of monomer (in grams per mole), Mw_{PMMA} = the molecular weight of monomer PMMA (in grams per mole), Mw_{MG49} = the molecular weight of monomer MG49 (in grams per mole), n_m = the total number of oxygen atom per repeated unit monomer (PMMA + MG49), n_{PMMA} = the number of oxygen atoms per repeated unit monomer PMMA, and n_{MG49} = the number of oxygen atoms per repeated unit monomer MG49.

The maximum and effective interaction for MG49:PMMA–LiBF$_4$ salt is [5/1] at the highest conductivity. This maximum conductivity value shows the maximum and effective interaction between oxygen atoms and Li$^+$ cations in the electrolyte. The interactions between Li$^+$ cations and

Table 1 [O/Li$^+$] ratios at different weight percent of LiBF$_4$ salt

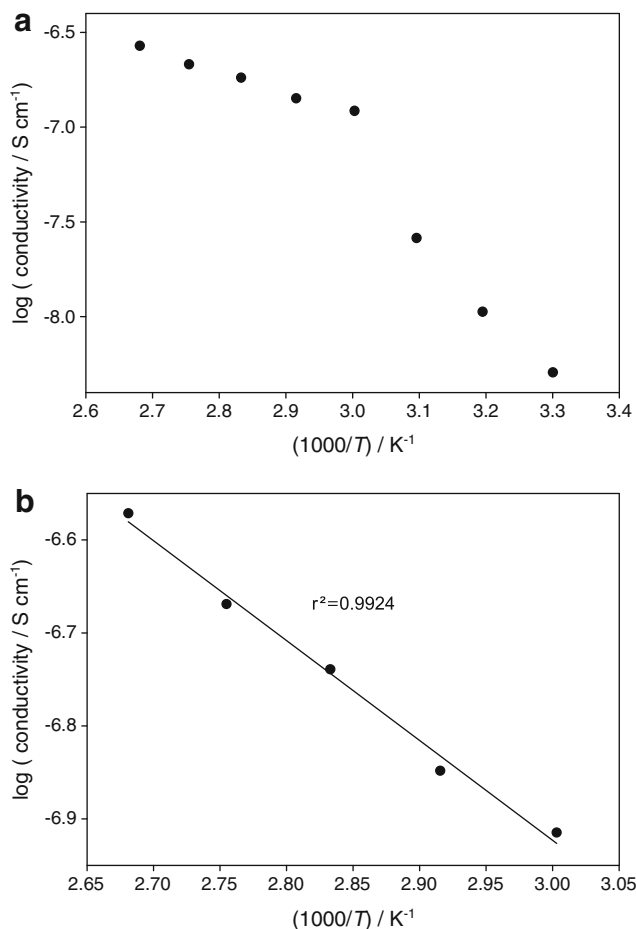| wt.% LiBF$_4$	[O/Li$^+$] ratio
0	–
5	26/1
10	13/1
15	9/1
20	6/1
25	5/1

Fig. 7 Temperature dependance of MG49:PMMA (30:70) at **a** 303–373 K and **b** 333–373 K

polymer host were proven by FTIR analysis as discussed earlier. According to Bruce in 2005, the structure of ether oxygen per Li consists of polymeric tunnels within that the Li^+ reside. The structure suggested the possibility of ion transport along the tunnels [34].

Figure 7a shows the temperature dependence of conductivity by the Arrhenius plot for the MG49:PMMA–LiBF$_4$. It was observed that the conductivity increased with the temperature from 303 to 373 K. The bulk resistance of the electrolyte could not be observed after 373 K since the sample was unstable at temperatures higher than 373 K. The relationship between conductivity and temperature was found to be linear in the temperature range from 333 to 373 K with the regression line of 0.992 as shown in Fig. 7b. This indicates that the electrolyte system exhibited Arrhenius-like behavior given by Arrhenius equation: $\sigma=\sigma_o e^{(-Ea/kT)}$, where σ_o, E_a, and k represent the pre-exponential factor, activation energy, and Boltzmann constant ($k=8.6\times10^{-5}$ eV K^{-1}), respectively [36]. The value for σ_o and E_a is calculated from the y-axis and plot intercept between log σ and 1,000/T [37]. $-E_a/kT$ is represented by the graph slope, m. From the Arrhenius plot, the activation energy E_a is 0.46 eV, while the pre-exponential factor σ_o is 1.21×10^{-7} S cm^{-1}.

The relationship between conductivity and temperature at range 303 to 323 K was found to be nonlinear with the correlation factor for the regression line is only 0.959. This indicates that the electrolyte system exhibited non-Arrhenius-like behavior in the temperature range from 303 to 323 K. This is the result of the β-relaxation of the PMMA segment as reported by Othman et al. [37]. The β-relaxation peak at 333 K was attributed to the main chain mobility below the glass transition temperature, T_g of PMMA. This indicates that the increase in segmental motion of the polymeric chain will also enhance the transport of ions in the polymer blend, resulting in the conductivity enhancement above the relaxation temperature, 333 K. The increase in the segmental motion of polymeric chain flexibility in the electrolyte leads to the increase in the dissociation rate of Li^+, thus improving the mobility of the charge carrier [38]. Despite the fact that the highest conductivity achieved by this electrolyte at this point, the value is still low to be applied in electrochemical devices as compared to the conventional system. However, this finding is the highest ionic conductivity at room temperature obtained in comparison to our previous studies on the series of MG49 [31], (70:30) MG49–PMMA [39], and (30:70) MG49–PMMA–LiClO$_4$ [23] blended solid polymer electrolytes. This result indicated that the increase in ionic conductivity was due to the increase of PMMA content. This was related to the increasing number of the coordinating sites contributed by oxygen atom in PMMA. The electron vacancy in oxygen atoms provided an alternative pathway for ions to be mobile from one site to another. Moreover, LiBF$_4$ salt gives a higher ionic conductivity in comparison to LiClO$_4$ because of the difference in anion size that affects the solubility of the salts [19, 31, 39].

Conclusions

A solid polymeric electrolyte of MG49:PMMA–LiBF$_4$ has been prepared by solution casting technique. The effect of LiBF$_4$ salt on the chemical interaction, structural, morphology, and conductivity of MG49:PMMA-based polymer electrolyte was investigated by FTIR, XRD, SEM, and AC impedance spectroscopy, respectively. The interaction between polymer host and lithium salt was confirmed by FTIR analysis. The shift was observed at δ(O–CH$_3$) asymmetric deformation of MMA from 1,461 to 1,456 cm^{-1}. XRD analysis suggested the crystallinity of PMMA is reduced by the addition of LiBF$_4$. The SEM results showed homogeneity of MG49:PMMA as no phase separation can be observed and recrystallization occurs as LiBF$_4$ content increases. From the impedance analysis, the conductivity was found to increase with the weight percent salt and reached the maximum value of 3.4×10^{-5} S cm^{-1} at 25 wt. % of LiBF$_4$ at room temperature due to the increase in the number of charge carrier. The electrolyte is Arrhenian in the temperature region from 333 to 373 K and not Arrhenian in lower temperature region from 303 to 323 K.

References

1. Chu PP, Reddy JM (2003) J Power Sources 115:288–294
2. Fenton DE, Parker JM, Wright PV (1973) Polymer 14:589
3. Chen YT, Chuang YC, Su JH, Yu HC, Chen-Yang YW (2011) J Power Sources 196:2802–2809
4. Rajendran S, Prabhu MR, Rani MU (2008) J Power Sources 180:880
5. Nair JR, Gerbaldi C, Destro M, Bongiovanni R, Penazzi N (2011) React Funct Polym 71:409
6. Stephan AM, Nahm KS (2006) Polymer 47:5952
7. Fergus JW (2010) J Power Sources 195:4554
8. Ahmad Sh, Ahmad Sf, Agnihotry SA (2004) J Power Sources 140:151–156
9. Chen HW, Lin TP, Chang FC (2002) Polymer 43:5281–5288
10. Ahmad A, Rahman MYA, Ali MLM, Hashim H, Kalam FA (2007) Ionics 13:67–70
11. Rajendran S, Mahendran O, Kannan R (2002) Fuel 81:1077–1081
12. Benedict TJ, Banumathi S, Veluchamy A, Gangadharan R, Ahmad AZ, Rajendran S (1998) J Power Sources 75:171–174
13. Idris R, Glasse MD, Latham RJ, Linford RG, Schlindwein WS (2000) J Power Sources 94:206–211

14. Park JW, Jeong ED, Won MS, Shim YB (2006) J Power Sources 160:674–680
15. Li W, Yang M, Yuan M, Tang Z, Zhang JQ (2007) J Appl Polym Sci 106:3084–3090
16. Wang XJ, Kang JJ, Wu YP, Fang FB (2003) Electrochem Commun 5:1025–1029
17. Latif F, Aziz AM, Katun N, Ali AMM, Yahya MZA (2006) J Power Sources 159:1401–1404
18. Alias Y, Ling I, Kumutha K (2005) Ionics 11:414–417
19. Kumutha K, Alias Y, Said R (2005) Ionics 11:472–476
20. Kumutha K, Alias Y (2006) Spectrochim Acta Part A 64:442–447
21. Ali AMM, Yahya MZA, Bahron H, Subban RHY (2006) Ionics 12:303–307
22. Ali AMM, Subban RHY, Bahron H, Winie T, Latif F, Yahya MZA (2008) Ionics 14:491–500
23. Su'ait MS, Ahmad A, Hamzah H, Rahman MYA (2009) J Phys D: Appl Phys 42:055410
24. Rajendran S, Uma T, Mahalingam T (1999) Ionics 5:232–235
25. Pavia DL, Lampman GM, Kriz GS (2001) Introduction to spectroscopy. Brooks/Cole, USA
26. Skoog DA, Holler FJ, Nieman TA (1998) Principle of instrumental analysis. Saunders College Publishing and Harcourt Brace College Publishing, CA, USA
27. Reddy MJ, Chu PP, Rao UVS (2006) J Power Sources 158:614–619
28. Subban RHY, Arof AK (2003) J New Mater Electrochem Syst 6:197–203
29. Baskaran R, Selvasekarapandian S, Kuwata N, Kawamura J, Hattori T (2006) Solid State Ionics 177:2679–2682
30. Ahmad A, Lien PC, Su'ait MS (2010) Sains Malaysiana 39:65–71
31. Su'ait MS, Ahmad A, Hamzah H, Rahman MYA (2009) Ionics 15:497–500
32. Loupy A, Tchoudar B (1991) Salts effects in organic and organic metallic chemistry. VCH, New York
33. Whang WT, Yang LH, Fan YW (1994) J Appl Polym Sci 54:923–933
34. Bruce PG (2005) Solid State Science 7: 1456–1463
35. Chew (2005) Kajian Kekonduksian Ionik Terhadap Adunan Elektrolit Polimer PVC-ENR dan PVdf-ENR. Thesis M.Sc Universiti Teknologi Malaysia, Malaysia
36. Noor SAM, Ahmad A, Talib IA, Rahman MYA (2010) Ionics 16: 161–170
37. Othman L, Chew KW, Osman Z (2007) Ionics 13:337–342
38. Rahman MYA, Ahmad A, Wahab SA (2009) Ionics 15:221–225
39. Su'ait MS, Ahmad A, Hamzah H, Rahman MYA (2011) Electrochim Acta 57: 123–131